

Photometric Observations with BYU-OPO Telescopes and APO's ARCSAT for Validation
of TESS Planetary Candidate Targets

Joe Williams

A senior thesis submitted to the faculty of
Brigham Young University
in partial fulfillment of the requirements for the degree of
Bachelor of Science

Denise Stephens, Advisor

Department of Physics and Astronomy
Brigham Young University

Copyright © 2026 Joe Williams

All Rights Reserved

ABSTRACT

Photometric Observations with BYU-OPO Telescopes and APO's ARCSAT for Validation of TESS Planetary Candidate Targets

Joe Williams

Department of Physics and Astronomy, BYU
Bachelor of Science

I have used telescopes from Brigham Young University's Orson Pratt Observatory (BYU-OPO) and Apache Point Observatory's (APO) Astrophysical Research Consortium Small Aperture Telescope (ARCSAT) to observe planetary candidates from the Transiting Exoplanet Survey Satellite (TESS). Working with the TESS Follow-up Observing Program (TFOP) Sub Group 1 (SG1), I have successfully observed transits of almost 100 planetary candidate objects. Mainly utilizing ARCSAT and the 24-inch BYU-OPO telescope, and given ideal weather conditions, I can confidently observe transits with a depth of at least 3 parts per thousand (ppt) in front of stars at least as bright as $V \approx 12$ magnitude. I have also been able to observe transits with depth of 4ppt and greater for stars as faint as $V \approx 14.5$ magnitude. I have also investigated relations between stellar parameters and calculated transit parameters for the targets observed and identified objects that have larger depths at bluer wavelengths. As I have observed exoplanet candidates, I have also observed previously uncatalogued variable stars, which will be characterized in the future.

Keywords: Exoplanets, Transit-detection, TESS

ACKNOWLEDGMENTS

I would like to acknowledge my research advisor, Dr. Denise Stephens, Dr. Eric Hintz who has helped with the BYU-OPO telescopes, the BYU Physics and Astronomy Department and College of Computational, Physical, and Mathematical Sciences. I would also like to acknowledge the Mount Cuba Astronomical Foundation who provided the grant to purchase the BYU-OPO 24-inch telescope. This research is also based on observations obtained with Apache Point Observatory's 0.5-m Astrophysical Research Consortium Small Aperture Telescope.

Contents

Table of Contents	iv
1 Introduction	1
2 Methods	4
2.1 Observing	4
2.1.1 ARCSAT	6
2.1.2 BYU-OPO	11
2.2 Data Processing	12
2.3 AIJ Photometry	12
3 Results	18
4 Discussion	22
4.1 ARCSAT	22
4.2 BYU-OPO 24-inch	23
4.3 Transit Parameters	24
4.4 Future Research	26
Appendix A Full Results Table	28
Bibliography	33
Index	35

Chapter 1

Introduction

The Transiting Exoplanet Survey Satellite (TESS) [1] is a space telescope that was launched in 2018 with the express goal of discovering exoplanets around stars in our nearby solar neighborhood using the transit detection method. This involves, as illustrated in Figure 1.1, observing a star and seeing how the incoming brightness from the star temporarily decreases by a small amount as the planet begins to eclipse its host star. The star then returns to its original brightness once the planet finishes eclipsing it. From the shape and size of this drop in light, we can begin to characterize the exoplanet, including its size relative to the star as well as the inclination of the orbit of the planet. The TESS satellite takes a series of wide field images of the same area of sky for a long period, hoping to see a drop in brightness and then return that could indicate a potential transiting planet. After an event has been observed by TESS, further validation of the presence of a transiting exoplanet requires follow-up observations by ground based telescopes to rule out potential false positives, refine the timing of a transit, and begin estimating parameters of the planet such as radius.

This work of identifying potential targets is currently being done, in part, by the TESS Follow-up Observing Program (TFOP) Sub Group 1 (SG1) [2]. Images from TESS are fed through MIT's Quick-look pipeline [3], identifying potential targets and initial estimates of orbital parameters. These potential targets, with their orbital parameters, are then added to a database for SG1 members

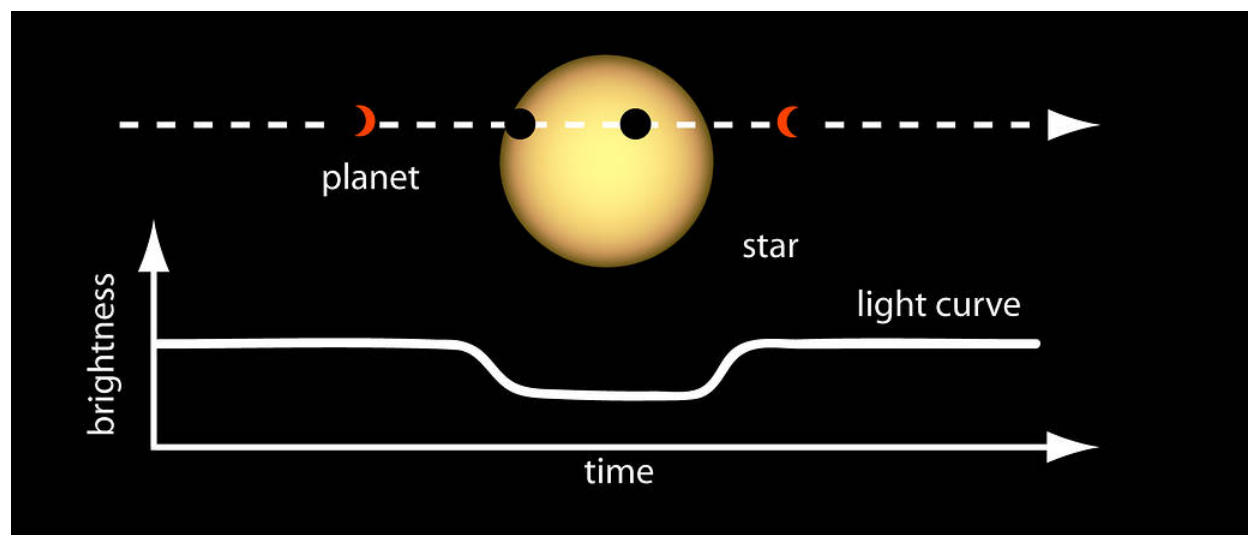


Figure 1.1 A visualization of a transiting exoplanet, blocking light as it passes in front of its host star and decreasing its brightness. Credit: NASA Ames

to observe with small ground-based telescopes, helping to validate these targets and refine parameters. This observation work by small ground-based telescopes is incredibly important, as large ground-based telescopes (>3m diameter) or spaced telescopes are needed for further confirmation and characterization of planet candidates, but time on these telescopes is much more valuable and their use needs to be optimized. Initial use of small ground-based telescopes to vet potential candidates and refine the timing of transit events leads to more efficient use of larger telescopes in confirming and characterizing exoplanets in the future.

With access to a 24-inch telescope at Brigham Young University's Orson Pratt Observatory (OPO) and remote access to Apache Point Observatory's (APO) 20-inch Astrophysical Research Consortium Small-Aperture Telescope (ARCSAT), I have established the effectiveness with which small ground based telescopes can be used in verifying transit events around TESS targets of interest [4], and refining of transit parameters. I have shown this, as I am a contributing member of TFOP SG1, with dozens of observations submitted to this group that confirm the detection of exoplanet candidates. And with the observation data I have taken, reasonable approximations

have also been established as to the limitations with which these telescopes can observe transiting exoplanets.

In this thesis, I will go through the process of selecting targets to observe, reducing my data, and then analyzing it to generate lightcurves for each object. Examples of some of these lightcurves will be included, and I have also included a full table containing calculated parameters for all of the transits that I have successfully observed. I will also show interesting relations between calculated transit parameters that show some insight into the population of exoplanet targets found by TESS.

Chapter 2

Methods

In order to achieve my results and produce full lightcurves for a multitude of objects, I conducted my own observations at the BYU-OPO 24-inch telescope or APO's 20-inch ARCSAT, and then processed all of the data. Methods and practices for each step of the data processing are laid out below, including a brief explanation of target selection, initial image processing, and then analysis and lightcurve generation with AstroImageJ [5].

2.1 Observing

As a member of the TESS Follow-up Observing Program (TFOP), I have access to a large database of targets that need further observations. The responsibility falls on observers to go through the database and select targets for each observing night. When choosing targets to observe, I make decisions based off the following, with their respective motivations:

- 1) *Predicted transit depth* - Larger drops in light, corresponding to a greater depth, are almost always easier to observe, and so my preference is to select the target with the greatest depth. Transit depths are measured in parts-per-thousand (ppt), where each part per thousand is a 0.1% drop in brightness

- 2) *Brightness of the host star* - The brighter a star is, the more light it gives off and so individual exposure times can be shortened when observing. This leads to better precision in determining the timing of events. Also, it's not common, but some stars can be too bright for my observations.
- 3) *Timing to maximize number of observations each night* - Not all targets require the entire night to observe the potential transit, and so I try to make choices that allow for multiple targets to be observed each night, when possible.
- 4) *Filters requested for observation* - Filters are used when observing to limit incoming light to certain wavelengths. Filter profiles, as seen in Figure 2.3 for SDSS filters [6] used on ARCSAT and Figure 2.4 for Johnson-Cousins filters [7] used for BYU-OPO telescopes, describe the wavelengths that each filter allows to pass through. Figure 2.3 also has different heights for each filter profile, which should be similarly be reflected in Johnson-Cousins filters. These different heights imply that some filters are more transparent for their wavelength regions and are more efficient for detecting incoming light. Filters that center on red and very near-infrared wavelengths, such as r' , i' , R , and I , tend to generally be the most transparent and so my preference is to use them and to gather the most amount of incoming light. Additionally, most of the stars that I observe happen to be redder, meaning that they give off more light in the wavelengths that these red and near-infrared filters are limited to. This makes it an even better decision to observe these targets in redder filters, and so most of my observations are done in r' or R , which will be apparent in the results section.
- 5) *Precision required for the observation* - For TFOP SG1, there are generally three possible goals when observing: an initial observation for a confirmation of an event, a high-precision observation in a red filter to refine timing, or high-precision observations in blue and/or infrared filters which help to rule out potential false positives. Reaching high precision requires receiving a lot of light from targets that and for the telescopes I have access to, is

usually only possible for very bright targets. Because of this, my preference has been to select targets that need observations to confirm events or refine timing of the event without a high-precision requirement.

- 6) *Proximity of other stars to the host star* - Most targets do not have any neighbors that are close enough that the stars overlap, but it does happen occasionally. If there is another star nearby, it can become difficult to isolate which star is the source of the event. Figure 2.1 shows an example of a target that has an overlapping neighbor, which has kept me from identifying which star is the source of the event. If at all possible, I do not select targets that have overlapping neighbors.

As shown in Figure 2.2, the TFOP target database contains information about each target, helping me to decide if it is adequate for observation. The number of observations able to be done each night changed throughout the year. In the winter, I was normally able to observe two or three separate targets, but in the summer, I could usually only observe one or two targets each night. I have already outlined some of my preferences when selecting targets, but each telescope also has limitations that determine the most appropriate targets for each telescope. Through my observing and processing of data from these telescopes, I have determined what these limitations are.

2.1.1 ARCSAT

With only remote access to Apache Point Observatory, my observing with ARCSAT is done virtually, but target selection is done through the TFOP database. For ARCSAT, given clear skies, targets selected:

- had a transit depth of at least 4ppt - larger drops are always better
- were stars of brightness between 10th and 14th magnitude - too bright and the stars would saturate leading to an inaccurate measure of the brightness, too faint and there wouldn't be enough incoming light

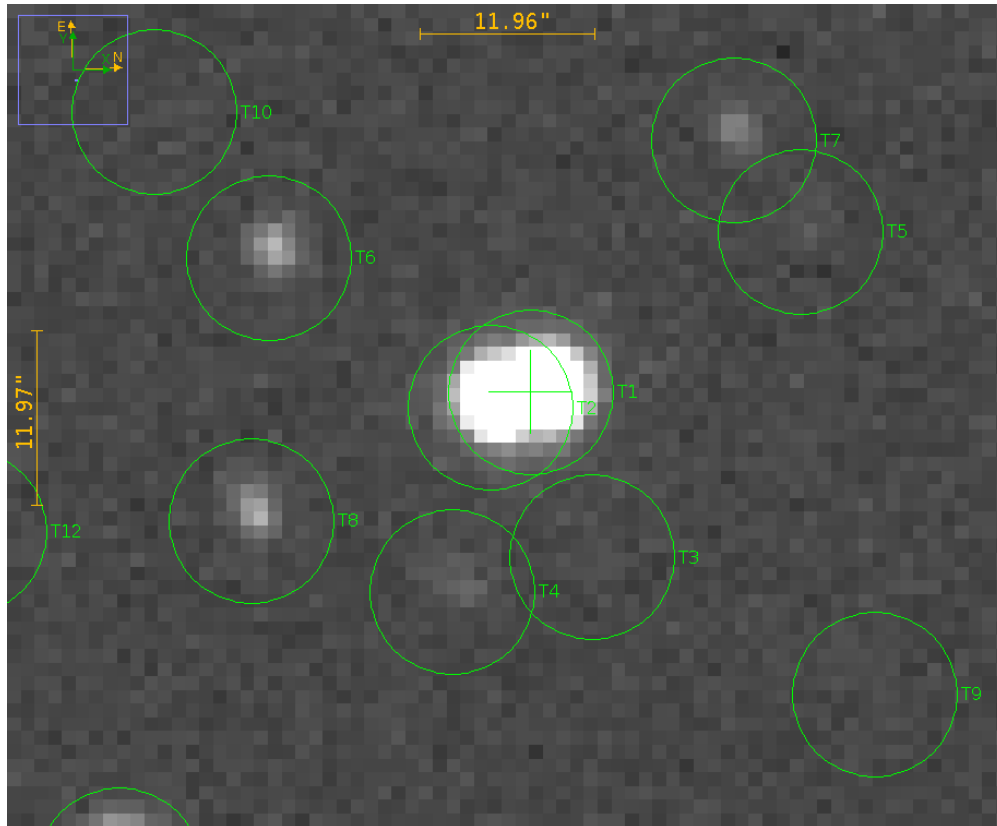


Figure 2.1 An example of a crowded field. Based on observations from TESS, SG1 believes that the star at the center of the circle labeled T1 is the source of the event, the right star in the overlapping pair. My observations confirmed that one of the two stars likely has a transiting planet, but I have not been able to determine exactly which star of the pair is the source.



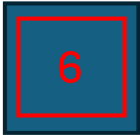
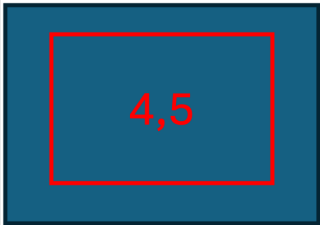
Local evening date	Name	V mag	T mag	Start—Mid—End	Duration	BJD _{TDB} start—mid—end	Elev. at start, mid, end ±1.0 hrs
Fri. 2026-01-30: Nautical twilight 2026-01-30 18:29 — 2026-01-31 06:03 local time / 2026-01-31 01:29 — 2026-01-31 13:0							
Fri. 2026-01-30 Nautical twilight 18:29 — 06:03 (America/Denver)	 Add to TOC Finding charts: Annotated , Aladin ; Info: ExoFOP , Simbad , Gaia , TIC , VSX , AIJ apertures , VizieR phot. ; Airmass , ACP plan	13.32	12.41	17:41 18:41— 19:19 —19:57 20:57 ±0:01	1:16 ±0:14 3	11071.5740 11071.6005 11071.6270	57° 67°, 73°, 77° 75°
% of transit (baseline) observable, Suggested obs. start, end	Az. at start, mid, end ±1.0 hrs	RA & Dec (J2000)	Period (days)	Depth (ppt)	Priority	R_{planet} (R_⊕)	Comments and followup status
3 UTC							
 100% (59%) 18:30—20:58	55° 49°, 38°, 16° 332°	 6	1.72	22.1 1	3	13.5	 4,5

Figure 2.2 An example of the information given for each target in the TFOP target database. This is usually one long row, but it has been split for visualizing better in print. Numbered boxes correspond to the priorities listed to help choose which targets to observe.

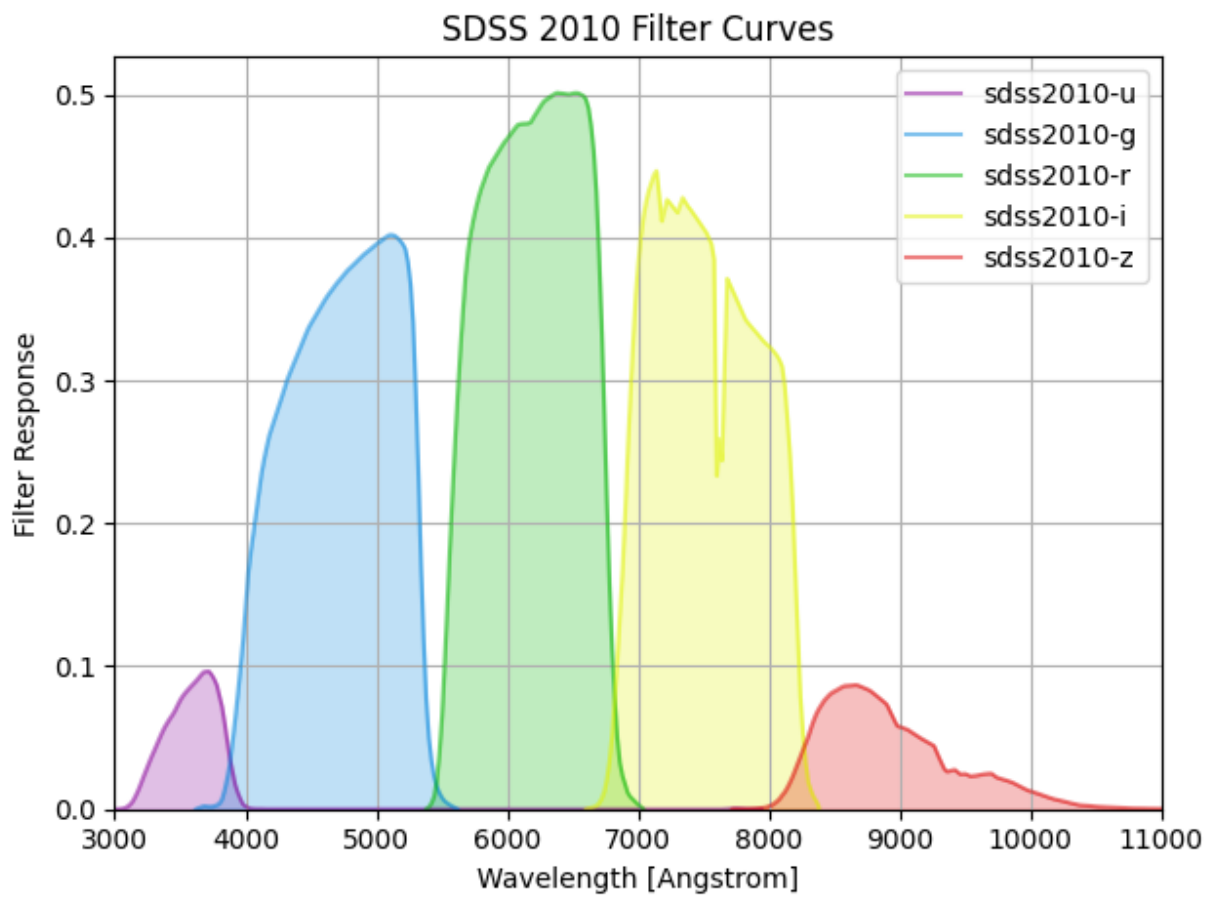


Figure 2.3 Filter profile for SDSS filters, used when observing with ARCSAT

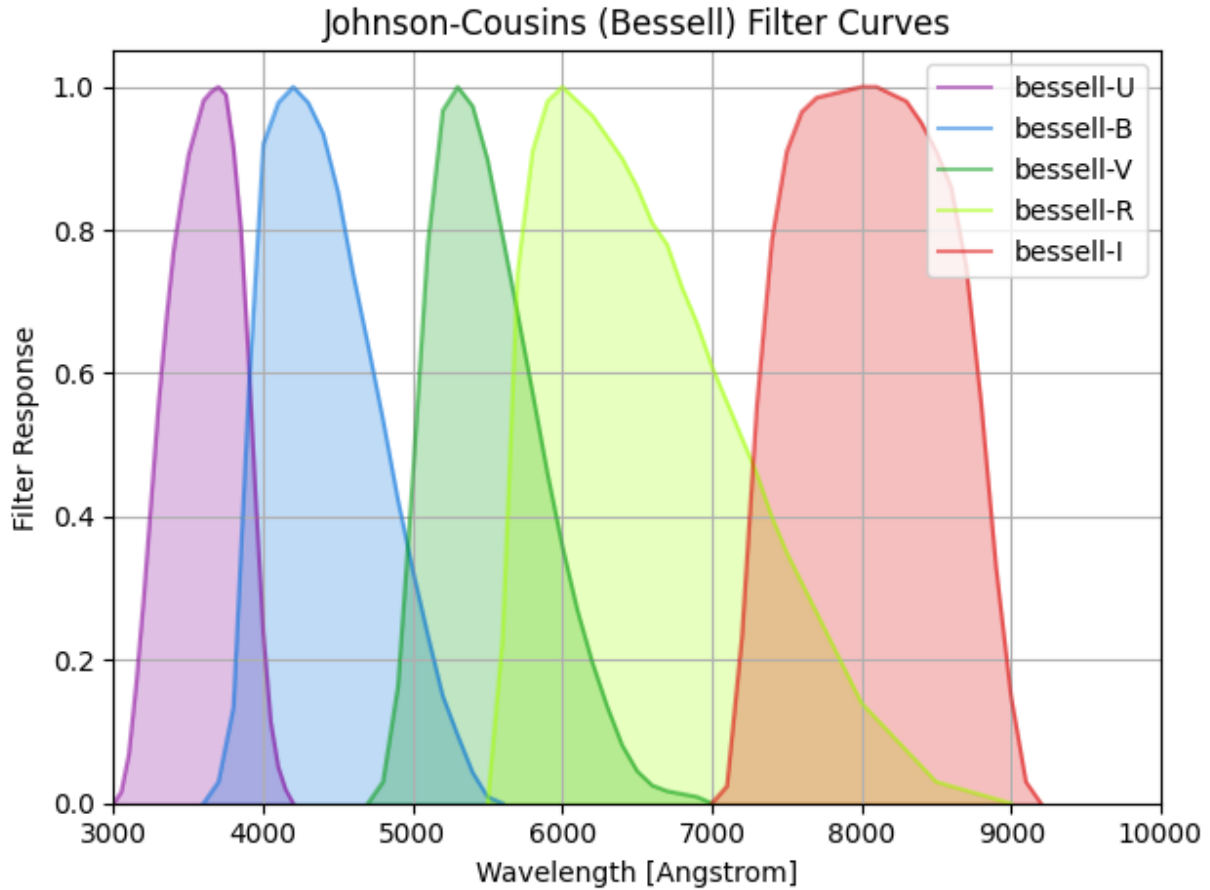


Figure 2.4 Filter profile for Johnson-Cousins (Bessell) filters, used when observing with BYU-OPO telescopes. The relative heights of the response curve for each filter has not been scaled as in Figure 2.3, but likely follows the same trend where the R filter would be the tallest, then decreasing in max height moving away from the center.

- needed observations in SDSS r' filter as a first choice, but g', i', and z' filters observations can also be performed
- were first-look observations that didn't require high-precision
- had at least four to five other stars in the star field that could be used as comparison stars in the data processing - more stars in the field is always preferable as it gives more options for comparison star, as long as these stars don't overlap with the target star

2.1.2 BYU-OPO

For the BYU-OPO 24-inch telescope, I have in-person access and so I personally run the programs to move the telescope and to take images. When selecting targets for this telescope, I use the same TFOP target database, but some preferences in target parameters differ because of the ability with this telescope to meet the TFOP high-precision requirement. Given clear sky conditions in Provo, these targets:

- were stars of brightness between 10th and 14th magnitude - the BYU-OPO 24-inch telescope is similar in size to ARCSAT and so the optimal stars to observe are the same brightness
- had a transit depth of at least 4ppt for any star, or if the star was brighter than 12th magnitude, a transit depth of 2ppt can also be observed - the noise is lower on observations with the 24inch and so I have been able to see smaller drops than with ARCSAT
- needed observations in Johnson R filter as a first choice, but B and I filter observations can also be performed - R filter lets more light through than B or I, and can be used for observations that don't need high-precision, so R more likely to be needed and preferable as a filter choice

There are less conditions that have to be met for targets to be observed with the 24-inch telescope due to its wider field image, whose observed area per image is approximately nine times that of ARCSAT's. For the other BYU-OPO telescopes, when I was using them for observations, my target selection was even more careful, with targets that:

- had brightness between 9th and 13th magnitude - smaller telescope and so brighter stars must be selected
- had a transit depth of at least 8ppt, but transit depths greater than 10ppt were preferred - noise is very high on measurements with these telescopes, and so only large drops are discernible
- needed observations in Johnson V or R filter - these filters allow the most light to pass through

2.2 Data Processing

General image processing is roughly the same for BYU-OPO telescope and ARCSAT observations. Basic image reduction to calibrate raw images is done through a custom Astropy script [8], after which any additional image header fields are added through IRAF [9], Barycentric Julian Dates (BJD) are added and any necessary plate-solving is done with the AstroImageJ (AIJ) software. These BJD dates are especially important as they serve as precise timing indicators of transit events, where the BJD represents the time that light from a star arrives at the solar system barycenter, and serves as the horizontal axis on all of my plots. After these steps, differential photometry is then performed using AIJ.

2.3 AIJ Photometry

Differential photometry is the process by which the brightness of a target star is compared over time with that of one or more comparison stars, hopefully showing that, relative to comparison stars which have a near constant brightness, our target star has a drop in brightness due to the transit event. All image sets require the use of AIJ to conduct differential photometry, though options for processing each dataset will differ depending on the filter used for observing, the star field of the object, and the weather and sky conditions of the observations. The first step is to estimate aperture sizes to perform photometry. For each star in the differential photometry process, each star has one

circular and one annulus aperture where the circular aperture is large enough to contain the pixels where most of the light comes in from the star, and the annulus just contains brightness from the background sky and this must be subtracted from the circular aperture. AIJ has an easy one-click step for suggesting the sizes of the circular aperture and the annulus. My suggested aperture sizes for stars are generally just larger than the typical FWHM of the target star. An example of the seeing profile generated can be found in Figure 2.5. After determining the aperture size, my next step is to find other stars in the field that have a near constant level of brightness, or flux. For my telescope, the flux is a measure of the number of photons incoming from the star to the detector over time. I will look at the whole star field and find stars that have incoming flux that is 0.5-1.0 times that of the target star. For ARCSAT, these comparison stars ideally have root-mean-square (RMS) scatter of $<5\text{ppt}$, and for the BYU-OPO 24-inch, these comparison stars have RMS scatter of $<3\text{ppt}$, or as low as 2ppt for bright target stars. Figure 2.6 is an example of a lightcurve plot comparing the target star with the comparison stars. As seen in Fig 2.2, the TFOP SG1 group provides estimates for the transit timing and period, and estimates of the host star parameters can be found using the Two Micron All-Sky Survey (2MASS), [10] which provides a J-K color that AIJ can use to approximate stellar parameters, such as the size of the star, its peak wavelength that it emits flux at, and its spectral type. These transit and host star parameters are adjustable through AIJ windows and heavily influence the predicted transit shape and planet size.

After selecting comparison stars, I then focus on the target star. Observing conditions, such as the sky brightness, star FWHM, total pixel count in the aperture, and more, can all change throughout the night and affect the differential photometry. AIJ can detrend by these parameters, and so even if conditions change throughout the night that would affect the target flux, these effects can be removed, ideally leading to a constant flux from the target star. When making a transit model, AIJ gives fit statistics, including the RMS, the chi-square, and the bayesian information criterion (BIC), which is related to the chi-square. A guide for the AIJ users in SG1 recommends that a detrend

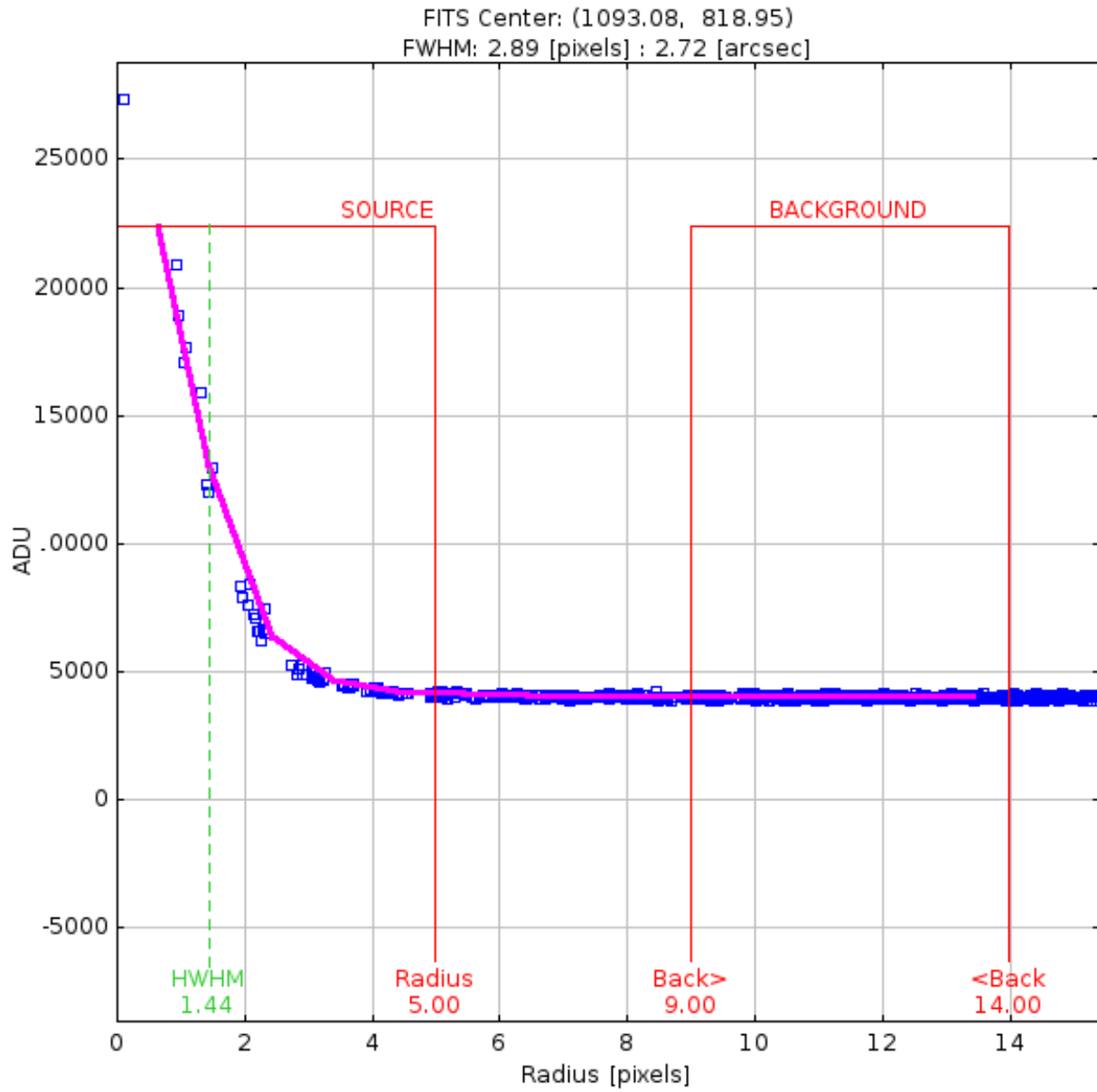


Figure 2.5 A seeing profile for very good observing conditions

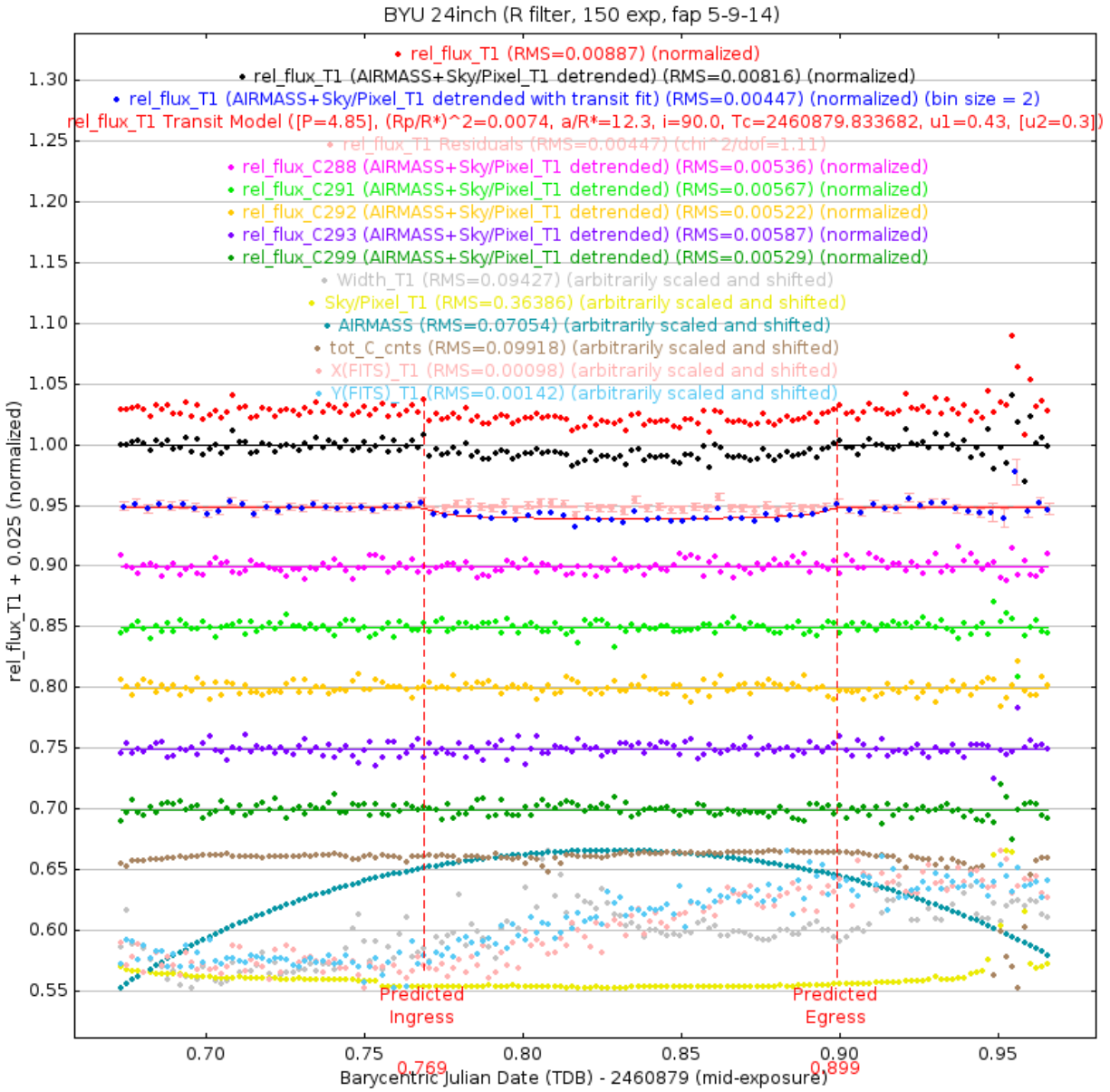


Figure 2.6 A seeing profile for very good observing conditions

parameter should be used if it decreases the BIC by 3 or more, and I have seen success in that yielding the best fits with my own data processing.

After detrending parameters have been selected, I look to find the optimal aperture size by varying the aperture size and finding the lowest RMS scatter on the target star's transit fit. I start from an aperture size of only a few pixels and then work up incrementally to a few pixels above the original suggested aperture size and eventually selecting the aperture size that yields the lowest RMS. After finding the best aperture size, I adjust the timing of the transit window to match the data instead of the predicted timing. After this, the processing is complete and a transit depth and time of center transit can be determined from the final plot that has been created, an example of which can be seen in Figure 2.7

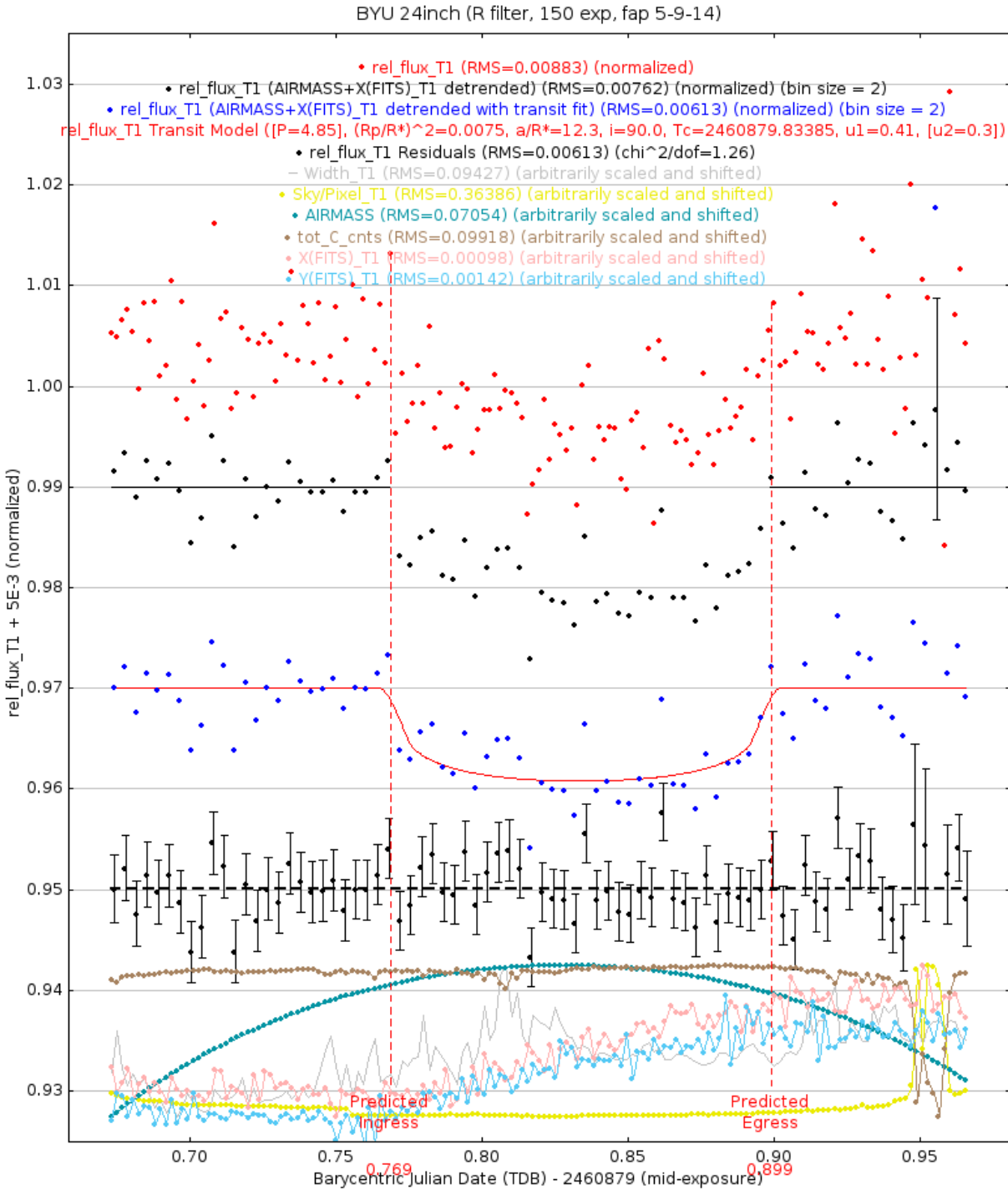


Figure 2.7 An example lightcurve, showing a transit occurring very close to the predicted window

Chapter 3

Results

As part of my collaboration with TFOP SG1, I cannot show individual targets names, but I will be presenting the basics of the transit parameters that have been found, and identify patterns with in target population. These results, which are constantly being updated, can be found in Appendix A. Each row in this table shows the date of observation, the telescope used for the observation, the filter, and the spectral type and J-K color of the star. After observing at the predicted interval and following the AIJ steps introduced previously, I have, for each object, determined a transit depth and planet size in Jupiter radii. After making all of these observations, I have created scatter plots showing correlations between the stellar parameters and calculated orbit parameters, with Figure 3.1 showing the transit depth compared to the J-K color, and Figure 3.2, which shows the correlation between planet size and transit depth. Additionally, I have included a plot of the spectral types for the host stars of the observations in Figure 3.3, which shows a large abundance of planets as orbiting G-type stars.

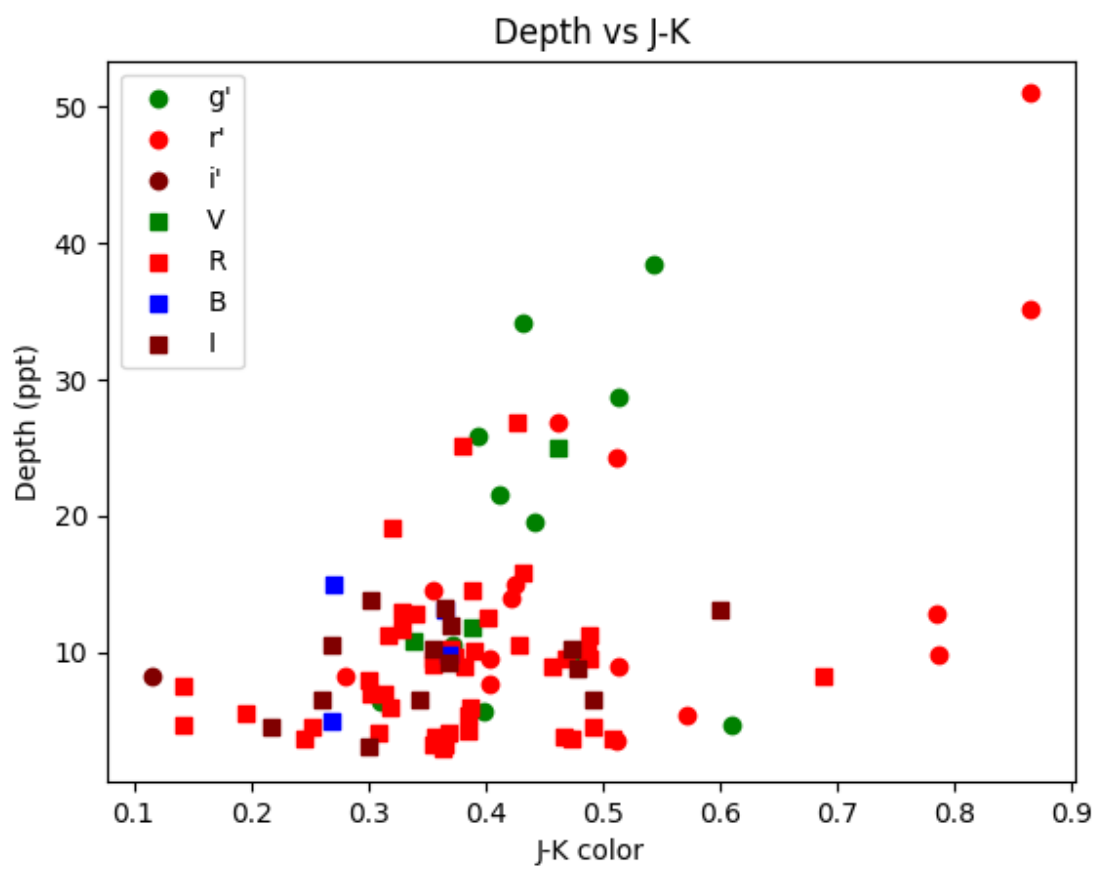


Figure 3.1 Scatter plot of transit depth and J-K color for the host stars

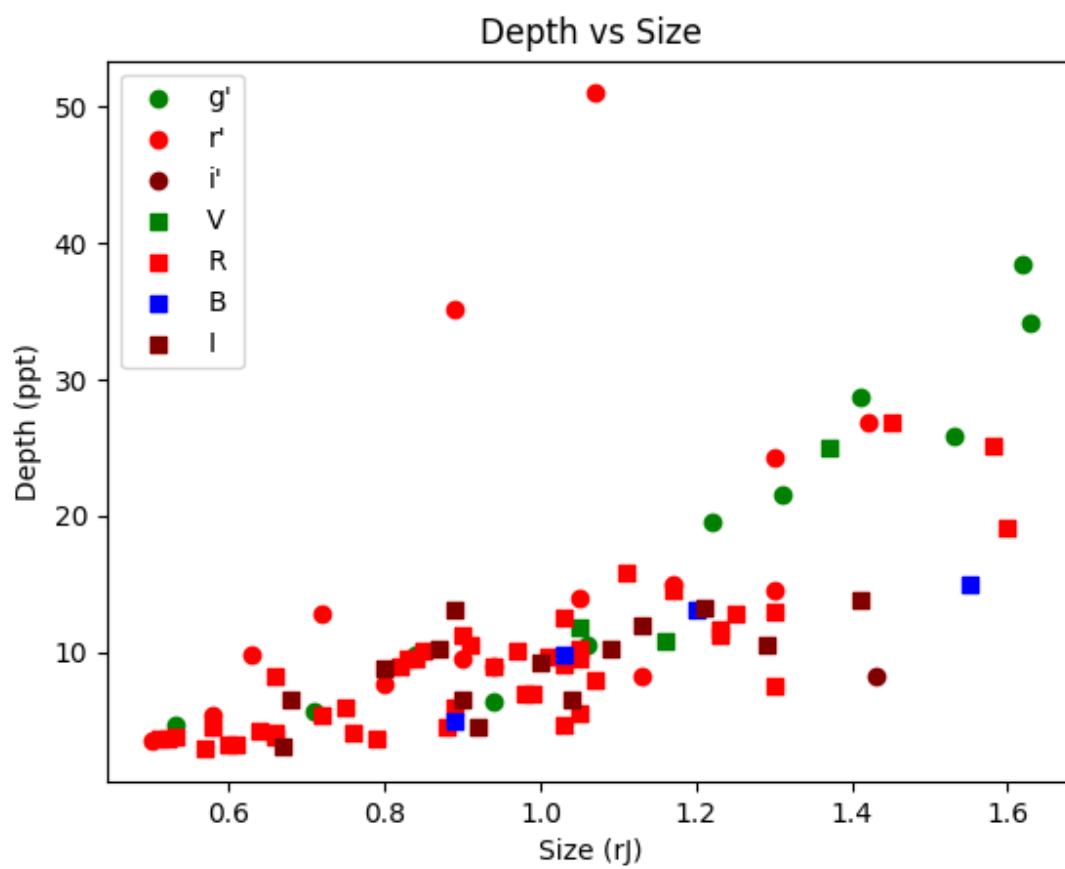


Figure 3.2 Scatter plot of transit depth and calculated planet size

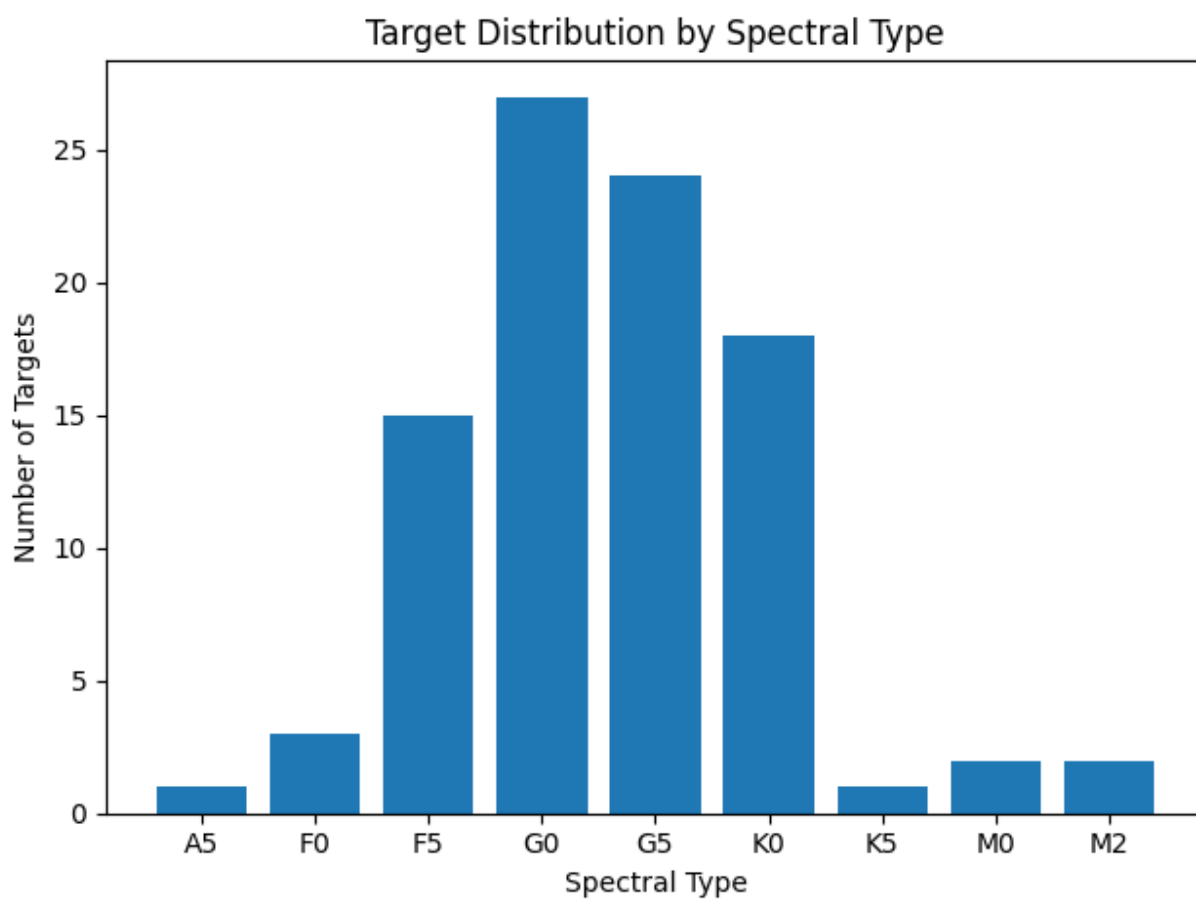


Figure 3.3 Spectral distribution of observed host stars

Chapter 4

Discussion

I have had access to four ground-based telescopes: APO's ARCSAT, and the BYU-OPO 24inch, 12inch, and 8inch telescopes. Due to their smaller sizes, the BYU-OPO 8inch and 12inch telescopes were not able to effectively observe most of the fainter targets provided by the SG1 group. The 8inch telescope was not used for any SG1 target observations, and the 12inch was only used for three observations that I was able to return to the group, which all were relatively deep drops. The BYU-OPO 24inch telescope and ARCSAT were more effective at observing SG1 targets, and so more discussion of their results is warranted and explained below.

4.1 ARCSAT

For ARCSAT in 2025, I was able to make 65 observations of TESS planetary candidates. Much of the data taken has yet to be processed as the BYU-OPO 24-inch telescope data is generally easier to process and yielded better results. Still, I have at least a dozen processed observations of TESS targets from ARCSAT this year. A fair number of these observations were conducted simultaneously with BYU-OPO 24inch, leading to a greater confidence that apparent drops in light were real and not just due to changing sky conditions or instrument errors. The best results from this year, so far,

include 1) a 6ppt drop in light and 2) 21ppt drop with current residuals of 2.9ppt/1min. For this second observation, the precision should increase if I bin the data points to a longer cadence. These observations define the effective limits for ARCSAT observations and thus help me select the best targets in the future. ARCSAT, as a 20inch telescope, is large enough to observe host stars as faint as 14th magnitude. It should be a viable option in order to observe transits at a high enough precision to send back to the TFOP group. However, only around 33% of observations with ARCSAT yielded data where I could clearly detect a transit event. For another 30% of the observations, the data was not precise enough to clearly observe an event or transits were not detected. For the remaining observations, technical errors prevented the data from being usable.

4.2 BYU-OPO 24-inch

In part due to its larger mirror size, it isn't surprising that the best data comes from observations on the BYU-OPO 24inch telescope. Currently, that is still the case, and so it has been the main focus of my efforts in processing data and submitting it to SG1. Since June 2025 when I started making observations on the 24inch telescope, I have made over 125 total observations of TESS targets, and that number continues to increase. There is still data to be processed for this telescope as well. However, of all of the data that has been processed so far from the 24-inch telescope, approximately 70% is conclusive in its results and of a high enough quality to be submitted to TFOP SG1. Another 20% of the observations are inconclusive and the final 10% is unusable due to either technical difficulties or unexpected weather issues. This fraction of usable data can hopefully be improved in the future, but already represents a larger amount of usable data compared to the other telescopes. In addition to a larger fraction of usable data, the quality of data obtained from observations with the 24-inch telescope is better than that of the other BYU-OPO telescopes or ARCSAT. Currently, our best results from the 24-inch are:

- a drop of 5.7ppt with residuals $<.95\text{ppt}/10\text{min}$
- no drop observed for a predicted depth of 3.1ppt, but residuals of $.62\text{ppt}/10\text{min}$, indicating we should have been able to observe the event if it had occurred
- a drop of 4.1ppt with residuals of $1.7\text{ppt}/5\text{min}$ for $V \approx 13$ magnitude

Through these observations and all others, I have also developed estimates for the quality of results to be expected when observing with clear skies. For 12th magnitude stars or brighter, I have observed transits down to 3ppt with residuals $<1\text{ppt}/5\text{min}$, the TFOP standard for high-precision. For stars fainter than this, down to 14th magnitude, I can confidently measure drops down to 4ppt with residuals around $1.5\text{ppt}/5\text{min}$.

4.3 Transit Parameters

I have generally made the decision to select targets that needed observations in red filter (r' and R) because they allow for the most transmission of light, generally leading to the best quality of data. Targets that need red filter observations also do not often require the SG1 high-precision standard, which I have struggled to consistently reach with any of the telescopes. With this reasoning, the vast majority of successful observations have been in these filters. After looking at the spectral distribution of all of the target host stars, it is also apparent that nearly all of the targets that I have observed are late F-type, G-type, or early K-type stars, which have a peak wavelength either at or just shorter than the wavelength band that the red filters most transparent to. Based on this distribution, the red filters are the best choice to make for attempting to confirm transit events or to attempt to reach high-precision.

When reviewing the scatter plot comparing the transit depths with calculated planet sizes, there is a clear linear trend that is to be expected, where larger planets lead to transit events with deeper drops in light. There is still some scatter from a very tight linear relationship because the size of the

host star can change as well, but this plot seems to support my intuition about how these parameters should be related. However, looking at the plot comparing the calculated depth of transit with the J-K color of the host stars, there is a grouping of stars that seems to show some unusual connection. As previously discussed, there is a greater abundance of G-type stars, which would correspond with J-K colors from around 0.3-0.5, and so there is a high density of data points in that region. Regardless of that grouping, most of the transits observed generally had a transit depth of 15ppt

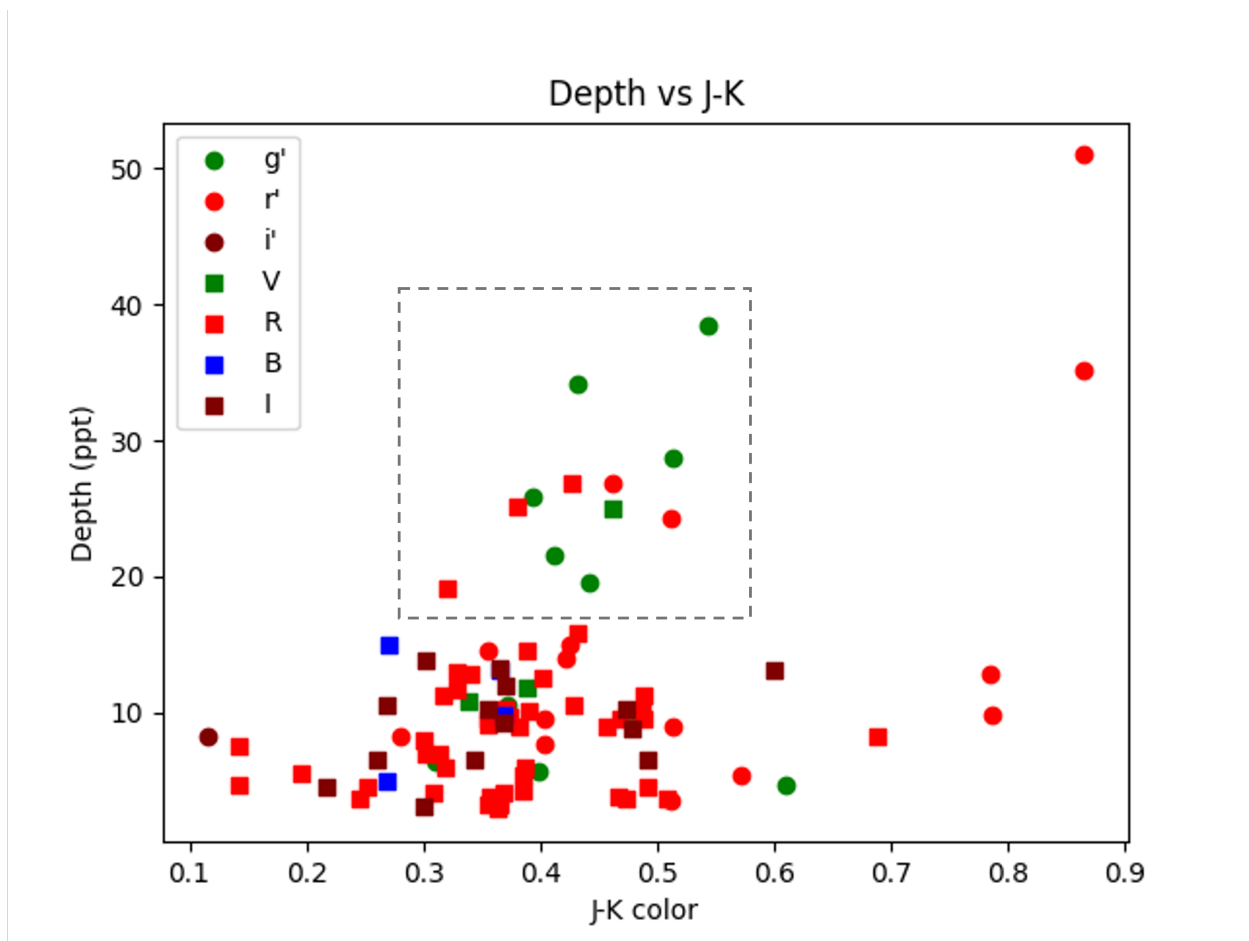


Figure 4.1 A lightcurve for one of the stars in the field of Target CP, which previously hasn't been identified.

or less, and so the points in the dashed box of Figure 4.1 highlight an odd grouping of targets that seem to have similar J-K colors or spectral types, but much deeper depth transit events. Most of the

observations that fall in this grey box are also taken with a bluer filter, g' or V , rather than a red filter. With this larger concentration of bluer filter observations that seems to coincide with unusually deep drops, there may be a need to make further observations of these targets to potentially rule out these targets as eclipsing binary rather than as exoplanet hosts, whose drop in light from a transit should be more invariant to filter choice.

4.4 Future Research

The TESS mission has continued to extend for multiple years and missions beyond original expectations [11]. As more data is continually gathered from TESS, new potential targets will be continually identified that need ground-based observations. Observations gathered from BYU telescopes have already been used by SG1 as part of the work by TFOP to validate TESS targets [12]. Future students will be able to continue the work that I have been performing and detect more transit events from TESS-QLP targets, to eventually be included in TFOP publications. I have also identified a grouping of objects in the Depth vs J-K color plot with a higher than normal fraction of observations in a bluer filter, which also have much deeper transit depths. Having both of these qualities, this grouping may be more likely to be made up of eclipsing binary systems rather than exoplanet hosts. This would take future observations, potentially again in these bluer filters, but potentially with different telescopes as well.

Aside from just observing exoplanets candidates, the time series photometry data also allows for discovery and analysis of other stars in the field of view with periodic fluctuations in brightness. This includes multiple types of variable stars and eclipsing binary systems. So far, I have been able to identify at least 20 potential variable stars that have not been cataloged or identified elsewhere. Future research could include further observations of these stars to confirm the periodic behavior and to begin to estimate a period. One such variable star that I have identified is in Figure 4.2.

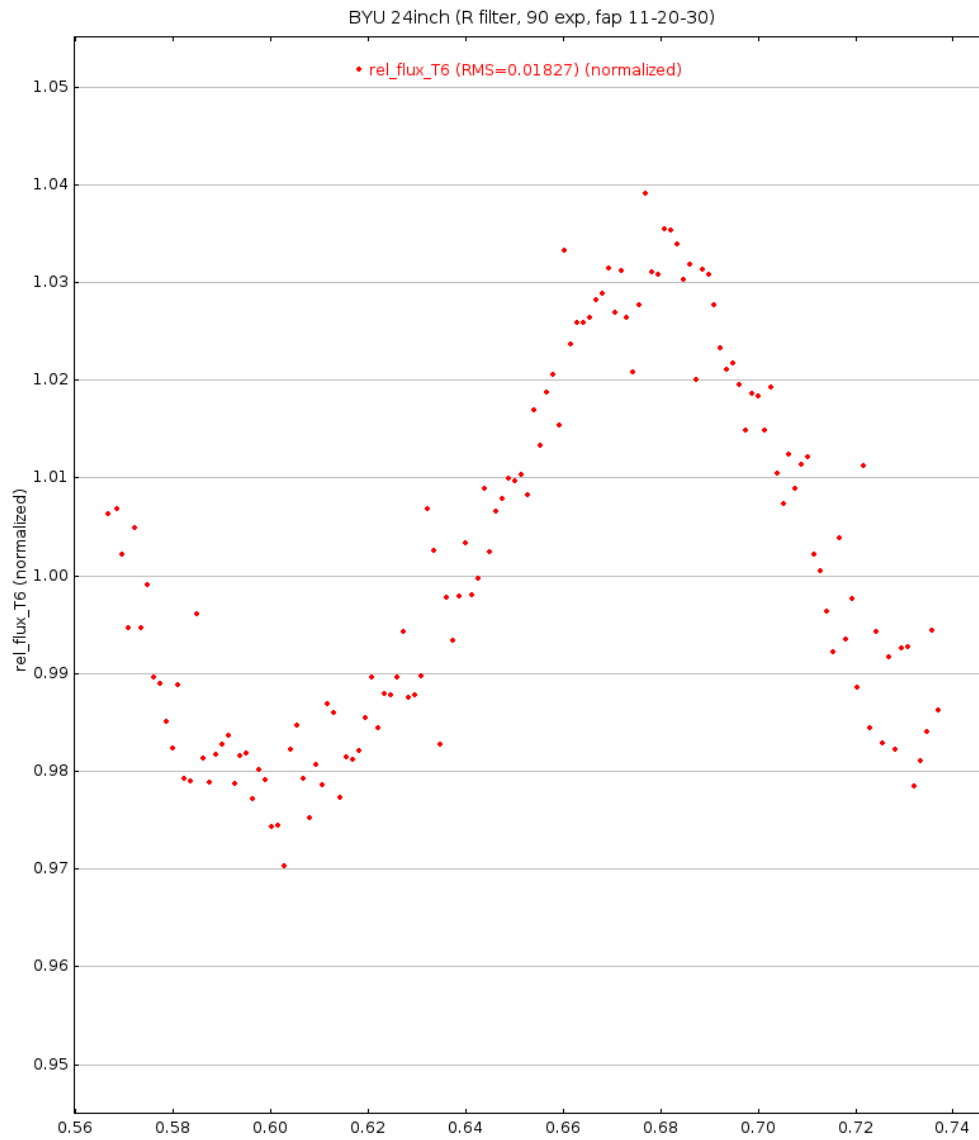


Figure 4.2 A lightcurve for one of the stars in the field of Target CP, which previously hasn't been identified.

Appendix A

Full Results Table

Table A.1 Transit Observations

Date (UT)	Target	Telescope	Filter	Depth (ppt)	Spectral Type	J-K Color	Planet Size (r_{Jup})
2024-12-03	AA	ARCSAT	g'	38.5	K0	.544	1.62
2024-12-09	AB	ARCSAT	g'	25.9	G5	.394	1.53
2024-12-10	AC	ARCSAT	g'	21.5	G5	.412	1.31
2024-12-14	AD	ARCSAT	g'	6.4	F5	.310	0.94
2024-12-16	AE	ARCSAT	g'	34.1	G5	.431	1.63
2024-12-19	AF	ARCSAT	g'	28.7	K0	.513	1.41
2024-12-21	AG	ARCSAT	g'	19.5	G5	.441	1.22
2024-12-24	AH	ARCSAT	r'	12.8	M0	.785	0.72
2024-12-25	AI	ARCSAT	g'	10.6	G0	.372	1.06
2024-12-29	AJ	ARCSAT	r'	8.3	F5	.281	1.13
2024-12-30	AK*	ARCSAT	r'	14.0	G5	.421	1.05
2024-12-30	AL	ARCSAT	i'	8.3	A5	.115	1.43
2025-01-07	AM	ARCSAT	r'	7.7	G5	.404	0.80

Date (UT)	Target	Telescope	Filter	Depth (ppt)	Spectral Type	J-K Color	Planet Size (r_{Jup})
2025-01-08	AN	12inch	V	25.0	G5	.461	1.37
2025-02-28	AN	ARCSAT	r'	26.8	G5	.461	1.42
2025-01-12	AO	ARCSAT	r'	35.2	M2	.865	0.89
2025-02-24	AO	ARCSAT	r'	51.0	M2	.865	1.07
2025-01-16	AP	12inch	V	11.9	G5	.389	1.05
2025-10-07	AP	24inch	R	14.5	G5	.389	1.17
2025-02-16	AQ	ARCSAT	g'	5.7	G5	.398	0.71
2025-02-17	AR	ARCSAT	r'	14.6	G0	.355	1.30
2025-02-20	AS*	ARCSAT	r'	15.0	G5	.425	1.17
2025-02-23	AT	ARCSAT	r'	9.8	M0	.786	0.63
2025-02-23	AU	12inch	V	10.8	G0	.338	1.16
2025-02-26	AV	ARCSAT	r'	3.5	K0	.511	0.50
2025-04-22	AV	ARCSAT	r'	24.3	K0	.511	1.30
2025-04-22	AW	12inch	R	26.8	G5	.427	1.45
2025-04-23	AX	ARCSAT	g'	9.8	K0	.483	0.84
2025-04-24	AY	ARCSAT	r'	5.4	K0	.572	0.58
2025-04-25	AZ	ARCSAT	g'	4.7	K0	.609	0.53
2025-04-26	BA*	ARCSAT	r'	9.6	G5	.403	0.90
2025-04-27	BB*	ARCSAT	r'	8.9	K0	.514	0.94
2025-06-03	BC	24inch	B	9.9	G0	.369	1.03
2025-06-03	BC	24inch	I	9.3	G0	.369	1.00
2025-06-04	BD*	24inch	R	15.8	G5	.432	1.11
2025-06-08	BE	12inch	R	12.8	G0	.341	1.25
2025-06-09	BF	12inch	R	10.1	K0	.487	0.85

Date (UT)	Target	Telescope	Filter	Depth (ppt)	Spectral Type	J-K Color	Planet Size (r_{Jup})
2025-06-10	BG	12inch	R	11.3	K0	.489	0.90
2025-06-14	BH*	24inch	R	10.3	G0	.371	1.05
2025-06-15	BI*	24inch	R	7.0	F5	.302	0.99
2025-06-18	BJ*	24inch	R	13.0	G0	.328	1.30
2025-06-21	BJ*	24inch	R	11.7	G0	.328	1.23
2025-06-19	BK	24inch	R	9.0	G5	.456	0.82
2025-06-20	BL	24inch	I	8.8	K0	.478	0.80
2025-06-29	BM*	24inch	R	10.1	G5	.390	0.97
2025-06-30	BN	24inch	I	3.1	F5	.301	0.67
2025-07-01	BO*	24inch	R	6.0	G0	.319	0.89
2025-07-11	BP	24inch	R	3.7	K0	.473	0.52
2025-07-12	BQ	24inch	I	13.1	K0	.600	0.89
2025-07-13	BR	24inch	I	13.9	F5	.302	1.41
2025-07-14	BS	24inch	I	10.2	G0	.355	1.09
2025-07-23	BT*	24inch	R	9.5	G5	.469	0.84
2025-07-27	BU	24inch	R	8.3	K5	.688	0.66
2025-07-28	BV*	24inch	R	8.0	F5	.300	1.07
2025-07-30	BW*	24inch	R	4.3	G5	.386	0.64
2025-08-04	BX*	24inch	R	3.7	F5	.246	0.79
2025-08-06	BY	24inch	B	5.0	F5	.269	0.89
2025-08-06	BY	24inch	I	10.5	F5	.269	1.29
2025-08-08	BZ*	24inch	R	9.5	G0	.355	1.05
2025-08-19	BZ*	24inch	R	9.1	G0	.355	1.03
2025-08-09	CA	24inch	R	7.5	F0	.143	1.30

Date (UT)	Target	Telescope	Filter	Depth (ppt)	Spectral Type	J-K Color	Planet Size (r_{Jup})
2025-08-13	CA	24inch	R	4.7	F0	.143	1.03
2025-08-18	CB	24inch	R	25.2	G0	.381	1.58
2025-08-20	CC*	24inch	R	11.2	G0	.317	1.23
2025-09-02	CD	24inch	I	6.6	G0	.343	0.90
2025-09-18	CE	24inch	R	3.8	G0	.357	0.66
2025-09-18	CF*	24inch	R	5.4	G5	.386	0.72
2025-09-23	CG*	24inch	R	12.5	G5	.402	1.03
2025-09-24	CH*	24inch	R	4.1	G0	.368	0.66
2025-09-25	CI*	24inch	R	2.9	G0	.364	0.57
2025-09-27	CJ*	24inch	R	3.7	K0	.508	0.51
2025-10-03	CK*	24inch	R	9.7	G0	.374	1.01
2025-10-09	CL	24inch	R	10.6	G5	.429	0.91
2025-10-13	CM	24inch	B	13.1	G0	.366	1.20
2025-10-13	CM	24inch	I	13.3	G0	.366	1.21
2025-10-19	CN	24inch	I	10.3	K0	.473	0.87
2025-10-21	CO	24inch	I	12.0	G0	.370	1.13
2025-11-01	CP	24inch	I	6.6	F5	.260	1.04
2025-11-03	CQ*	24inch	R	5.6	F0	.195	1.05
2025-11-05	CR*	24inch	R	6.0	G5	.387	0.75
2025-11-07	CS	24inch	I	6.5	K0	.491	0.68
2026-02-06	CS	24inch	R	4.6	K0	.491	0.58
2025-11-08	CT	24inch	I	4.6	F5	.217	0.92
2025-11-09	CU*	24inch	R	9.0	G0	.382	0.94
2025-11-10	CV*	24inch	R	3.8	G5	.467	0.53

Date (UT)	Target	Telescope	Filter	Depth (ppt)	Spectral Type	J-K Color	Planet Size (r_{Jup})
2025-11-10	CW*	24inch	R	7.0	F5	.314	0.98
2025-11-26	CX	24inch	R	3.2	G0	.355	0.61
2025-11-27	CY*	24inch	R	4.6	F5	.252	0.88
2025-11-27	CZ	24inch	R	9.5	K0	.489	0.83
2026-01-15	DA*	24inch	R	3.3	G0	.365	0.60
2026-02-05	DB*	24inch	R	19.1	G0	.320	1.60
2026-02-05	DC*	24inch	R	4.1	F5	.309	0.76
2026-03-12	DD	24inch	B	15.0	F5	.271	1.55

* Indicates a first-look observation.

Bibliography

- [1] G. R. Ricker *et al.*, “The Transiting Exoplanet Survey Satellite,” *Journal of Astronomical Telescopes, Instruments, and Systems* **1**, 014003 (2015).
- [2] K. A. Collins, “The TESS Follow-up Observing Program Working Group,” In *American Astronomical Society Meeting Abstracts*, **233**, 140.05 (2019).
- [3] M. Kunimoto, J. N. Winn, G. R. Ricker, and R. K. Vanderspek, “Predicting the Exoplanet Yield of the TESS Prime and Extended Missions Through Years 1–7,” *The Astronomical Journal* **163**, 290 (2022).
- [4] N. M. Guerrero *et al.*, “The TESS Objects of Interest Catalog from the TESS Prime Mission,” *The Astrophysical Journal Supplement Series* **254**, 39 (2021).
- [5] K. A. Collins, J. F. Kielkopf, K. G. Stassun, and F. V. Hessman, “AstroImageJ: Image Processing and Photometric Extraction for Ultra-Precise Astronomical Light Curves,” **153**, 77 (2017).
- [6] M. Doi *et al.*, “Photometric Response Functions of the Sloan Digital Sky Survey Imager,” *The Astronomical Journal* **139**, 1628–1648 (2010).
- [7] M. S. Bessell, “UBVRI passbands,” *Publications of the Astronomical Society of the Pacific* **102**, 1181–1199 (1990).

-
- [8] Astropy Collaboration *et al.*, “Astropy: A community Python package for astronomy,” **558**, A33 (2013).
- [9] D. Tody, “The IRAF Data Reduction and Analysis System,” In *Instrumentation in Astronomy VI*, D. L. Crawford, ed., Proceedings of the SPIE **627**, 733 (1986).
- [10] M. F. Skrutskie *et al.*, “The Two Micron All Sky Survey (2MASS),” **131**, 1163–1183 (2006).
- [11] G. R. Ricker *et al.*, “The Transiting Exoplanet Survey Satellite (TESS): Mission Overview and Status,” *Bulletin of the American Astronomical Society* **54**, 020 (2022).
- [12] S. W. Yee *et al.*, “The TESS Grand Unified Hot Jupiter Survey. III. Thirty More Giant Planets,” *The Astrophysical Journal Supplement Series* (2025), in press / submitted.

Index

AIJ, 4, 12
APO, 2
 ARCSAT, 2, 4, 6, 22
BYU-OPO, 2, 4, 11, 23
Lightcurve, 3, 16
QLP, 1
SG1, 1, 18
TESS, 1, 26
TFOP, 1, 4, 18